Pressure dependence of the superconducting critical temperature of $Tl_2Ba_2Ca_2Cu_3O_{10+y}$ and $Tl_2Ba_2Ca_3Cu_4O_{12+y}$ up to 21 GPa

D. Tristan Jover, R. J. Wijngaarden, and R. Griessen
Department of Physics and Astronomy, Free University, De Boelelaan 1081, 1081 HV Amsterdam, The Netherlands

E. M. Haines and J. L. Tallon
Institute for Industrial Research & Development, Gracefield Research Centre, Gracefield Road, P.O. Box 31310, Lower Hutt, New Zealand

R. S. Liu
Department of Chemistry, National Taiwan University, Roosevelt Road, Section 4, Taipei, Taiwan, Republic of China

(Received 30 November 1995; revised manuscript received 5 April 1996)

Using a cryogenic diamond anvil cell (DAC) the pressure dependence of the superconducting transition temperature T_c of $Tl_2Ba_2Ca_2Cu_3O_{10+y}$ (Tl-2223) and $Tl_2Ba_2Ca_3Cu_4O_{12+y}$ (Tl-2234) has been measured resistively up to 21 GPa. At ambient pressure these compounds have T_c's of 128.5 K and 113 K. At low pressures, the pressure dependence $\partial T_c/\partial p$ is 1.75 K/GPa in Tl-2223 and 2.0 K/GPa in Tl-2234. As pressure is increased T_c continues to increase (although the rate diminishes) until T_c reaches a maximum of 133 K at 4.2 GPa in Tl-2223 and of 120 K at 6.6 GPa in Tl-2234. At higher pressures T_c decreases. In this region a rather abrupt change in $\partial T_c/\partial p$ is observed at $p_c=12.0$ GPa in Tl-2223 and at $p_c=10.5$ GPa in Tl-2234. The kink at p_c is interpreted as an indication of the presence of *inequivalent* CuO_2 layers: Below p_c the T_c of the samples is determined by the intrinsic T_c of the outer CuO_2 layers while above p_c it is determined by that of the inner CuO_2 layers. [S0163-1829(96)07134-2]

I. INTRODUCTION

Superconductivity in high-T_c superconductors is generally regarded as a property of CuO_2 layers. The number n of CuO_2 layers per chemical formula unit may vary within a homologous series: For $Tl_2Ba_2Ca_{n-1}Cu_nO_{2n+4+y}$ bulk samples with $n=1$, 2, 3, and 4 have been synthesized. In the $n=2$ compound both CuO_2 layers per half unit cell are crystallographically *equivalent*. However, in the $n=3$ and $n=4$ compounds, shown schematically in Fig. 1, there are two different kinds of CuO_2 layers: the inner (i) CuO_2 layer(s) and the outer (o) CuO_2 layers which are crystallographically *inequivalent*. An interesting question which immediately arises is whether the presence of inequivalent CuO_2 layers leads to characteristic features in the physical properties of these compounds. Trying to find an answer to this question was the main motivation for the experimental work described in this paper. In order to bring forward the *intrinsic properties* of the *inequivalent* CuO_2 layers external pressure is used. The application of pressure has proved to be a most useful means of changing the charge carrier or hole concentration n_h, defined as the number of holes per copper atom, on the CuO_2 layers. By changing the charge carrier density n_h also T_c is changed and hence pressure is (as will be detailed below) a means to change the intrinsic T_c of the inequivalent CuO_2 layers in a different manner. From chemical doping experiments a clear picture has emerged in which T_c varies almost parabolically with the hole concentration.[1] For $La_{2-z}Sr_zCuO_4$, as well as several other cuprates, it appears that optimal doping occurs for[1–3] $n_h=0.16$. Compounds with a lower hole concentration are said to be *underdoped* while compounds with a higher hole concentration are said to be *overdoped*. In the rest of this article it is assumed that this parabolic dependence presents a reasonable description of the superconducting phase diagram of the CuO_2 layers. All that appears to vary from one compound to another is the value of $T_{c\max}$, the maximum T_c attainable, which correlates closely with the state of stress of the CuO_2 layers[2] but depends in principle also upon interlayer coupling, as for example in the resonating valence bond (RVB) model[4] or the van Hove singularity scenario,[5,6] and the nature of the charge reservoir layers.

Where there exists a charge reservoir such as the TlO layers in the thallium–based high–T_c superconductors, the application of pressure appears to transfer charge from the charge reservoir to the CuO_2 layers due to the contraction of the Cu- (apical) O bond length which favors removal of antibonding electrons. Thus, pressure raises the hole concentration on the CuO_2 layers which explains the similarity between pressure and doping experiments. Assuming that the intrinsic effect of pressure on $T_{c\max}$ is neglible this simple model implies that for compounds in the underdoped (overdoped) region $\partial T_c/\partial p$ is positive (negative), while at optimal doping $\partial T_c/\partial p$ is zero. A large number of compounds indeed exhibit a parabolic dependence of T_c upon pressure. Due to the small pressure dependence of $T_{c\max}$, however, $\partial T_c/\partial p$ is often found to be positive for optimally doped compounds. A general overview of high-pressure experiments is given by Wijngaarden and Griessen,[7] Schilling and Klotz,[8] and recently also by Takahashi and Môri.[9] For compounds with *inequivalent* CuO_2 layers a more complicated behavior is expected.[10] In the simplest case the inner and

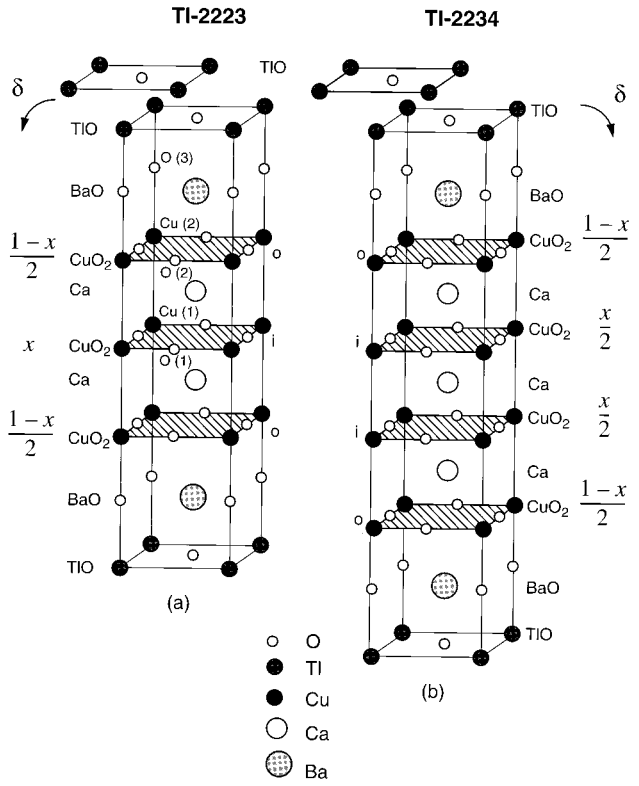

FIG. 1. Idealized structures of (a) Tl-2223 and (b) Tl-2234 with, respectively, three ($n=3$) and four ($n=4$) CuO_2 layers per half unit cell. Both structures have *inequivalent* inner (i) and outer (o) CuO_2 layers. While the copper atoms of the inner CuO_2 layer(s) have a fourfold oxygen coordination, the copper atoms of the outer CuO_2 layers have a fivefold oxygen coordination.

outer CuO_2 layers follow a different parabolic $T_c(n_h)$ curve, different in the sense that they are shifted with respect to each other, since the charge carrier density n_h of these layers may not be the same.

The first indication of such behavior was in the experiment by Berman *et al.*[10] on a Tl-2223 sample with, at ambient pressure, a T_c of 104 K. Using a Bridgman anvil cell they observed up to 7 GPa a linear increase in T_c at a rate of 1.2 K/GPa. At higher pressures T_c reached a maximum and started to decrease. After going through a minimum in the range 13–15 GPa, T_c started to increase again. On decreasing pressure the same behavior was observed. The authors explain their results by supposing that there might be a structural phase transition. In the x-ray experiments of Fietz *et al.*,[11] however, no such transition is observed. The experiment by Berman *et al.*[10] may therefore have been the first to show the effect of inequivalent CuO_2 layers. There are a few other experiments on Tl-2223. Under hydrostatic conditions Kubiak *et al.*[12] found, in an experiment to 1 GPa, an increase in T_c at a rate of 5.0 K/GPa. In two overdoped samples, Berkley *et al.*[13] increased T_c from 116 K at ambient pressure to 132 K at 7 GPa, with at low pressures a $\partial T_c/\partial p$ of 4.8 K/GPa. In two optimally doped Tl-2223 samples the same group found a value of 0.7 K/GPa. For a further discussion the reader is referred to the review articles mentioned above.

This paper is organized as follows. In Sec. II two relevant phenomenological models are considered in order to describe $T_c(n_h)$ and $T_c(p)$ for the $n=3$ and $n=4$ thallium-based high-T_c compounds. In the first model, the *sheet-charge model*, the charge on the CuO_2 layers is assumed to be distributed uniformly even when the charge distribution among the CuO_2 layers is not homogeneous. In the second model, the *point-charge model*, a more ionic approach is taken. After a description of the sample preparation and the experimental details in Secs. III and IV, high-pressure results on Tl-2223 and Tl-2234 samples are presented and discussed in Sec. V.

II. PHENOMENOLOGICAL MODELS

To model $T_c(p)$ for compounds with *inequivalent* CuO_2 layers the following scheme will be used. Pressure induces a charge transfer from the TlO layers towards the CuO_2 layers. The distribution of this charge between the CuO_2 layers is calculated using two different models: (i) the model of Di Stasio, Müller, and Pietronero[14] and (ii) the model of Haines and Tallon.[15] Once the charge carrier density n_h of each CuO_2 layer is found, its normalized intrinsic T_c is calculated from the known parabolic $T_c(n_h)$ dependence, and finally using either proximity coupling or no coupling at all, the resulting T_c of the compound as a whole is calculated. This section starts with a discussion of the two models to calculate the charge distribution among the *inequivalent* CuO_2 layers.

A. Model of Di Stasio, Müller, and Pietronero

A first attempt to calculate the charge distribution among the *inequivalent* CuO_2 layers was made by Di Stasio *et al.*[14] using a simple model in which noninteracting holes are confined to the square CuO_2 layers, thus forming two-dimensional sheets of charge. In their model the charge is distributed uniformly on the CuO_2 layers. Assuming that a *fraction* x of the total number δ of holes transferred from the TlO charge reservoir layers resides on the inner CuO_2 layer(s), a *fraction* $1-x$ has to reside on the outer CuO_2 layers (see Fig. 1).

The total electron energy $U_{\rm tot}$ per formula unit, or in this case per half unit cell, is then defined as the sum of a band energy U_b and an electrostatic energy $U_{\rm es}$:

$$U_{\rm tot}=U_b+U_{\rm es}. \tag{1}$$

For a particular CuO_2 layer the band energy is given by

$$U_b=\frac{\pi\hbar^2}{2m^*a^2}n_{hi}^2, \tag{2}$$

where n_{hi} is the charge carrier density of the ith CuO_2 layer given by

$$n_{hi}=\frac{x}{n-2}\,\delta \text{ for the inner } CuO_2 \text{ layer(s)},$$

$$n_{hi}=\frac{1-x}{2}\,\delta \text{ for the outer } CuO_2 \text{ layers}, \tag{3}$$

m^* is the effective mass of the noninteracting holes in a parabolic CuO_2 band, and a is the lattice parameter of the *square* CuO_2 layer.

The electrostatic energy of a pair of charged layers is given by

$$U_{\rm es}=-\frac{e^2}{2}\frac{n_{hi}n_{hj}}{C_{ij}}, \tag{4}$$

where e is the electron charge,

$$C_{ij}=\frac{\epsilon a^2}{4\pi|i-j|d_0} \tag{5}$$

is the sheet capacitance of the ith layer with respect to the jth layer, ϵ is the background dielectric constant due to the charge carriers which are not included in the parabolic CuO_2 bands, and d_0 is the distance between adjacent CuO_2 layers. For simplicity the distance between the charge reservoir layers and that between one of these layers and the nearest CuO_2 layer is also taken to be d_0. After summation over all the relevant layers Eqs. (2) and (4) yield for the $n=3$ and 4 structures, respectively,

$$U_b(x)=\frac{\pi\hbar^2}{2m^*a^2}\delta^2\left(\frac{3x^2}{2}-x+\frac{1}{2}\right) \quad \text{for } n=3,$$

$$U_b(x)=\frac{\pi\hbar^2}{2m^*a^2}\delta^2\left(x^2-x+\frac{1}{2}\right) \quad \text{for } n=4, \tag{6}$$

and

$$U_{\rm es}(x)=\frac{\pi d_0e^2}{\epsilon a^2}\delta^2(x^2+3) \quad \text{for } n=3,$$

$$U_{\rm es}(x)=\frac{\pi d_0e^2}{2\epsilon a^2}\delta^2(2x^2+7) \quad \text{for } n=4. \tag{7}$$

Minimizing the total band energy U_b with respect to x obviously leads to a homogeneous charge distribution with $x=1/3$ for $n=3$ and $x=1/2$ for $n=4$. This, of course, corresponds to the minimum of $U_b(x)$. The electrostatic energy, which favors maximal charge separation ($x=0$), is therefore responsible for nonhomogeneous charge distributions in these layered structures. The minimum in the total energy $U_{\rm tot}$ is found to occur at

$$x_{\rm min}=\frac{1}{3+2A_s} \quad \text{for } n=3,$$

$$x_{\rm min}=\frac{1}{2(1+A_s)} \quad \text{for } n=4, \tag{8}$$

where A_s is defined as

$$A_s=2\frac{m_ee^2}{\hbar^2}d_0\frac{m^*/m_e}{\epsilon}. \tag{9}$$

Following Di Stasio *et al.*,[14] by taking $d_0=3.1$ Å and $(m^*/m_e)/\epsilon\simeq 0.33$, a value of approximately 4 is obtained for A_s. Substituting this value in Eq. (8) shows that according to this model the charge distribution in both Tl-2223 and Tl-2234 is highly nonhomogeneous with a fraction of ~ 0.1 of the holes in the inner CuO_2 layer(s) and thus a fraction of ~ 0.9 of the holes in the outer CuO_2 layers. So far it has been assumed that at ambient pressure δ has a value of 0.45

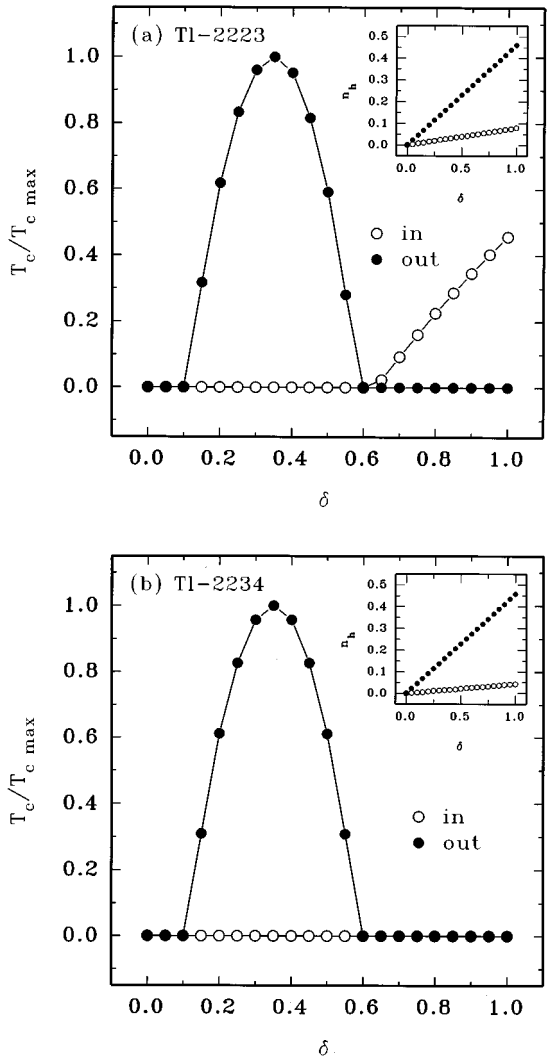

FIG. 2. Normalized T_c values in the model of Di Stasio, Müller, and Pietronero (Ref. 14) for the inner and outer CuO_2 layers as a function of the total number δ of holes transferred from the TlO charge reservoir layers to the CuO_2 layers in (a) Tl-2223 and (b) Tl-2234 based on Eq. (10) and the calculated charge distribution as shown in the insets taking $(m^*/m_e)/\epsilon\simeq 0.33$.

for Tl-2223 as well as for Tl-2234. Since Eq. (8) does not depend explicitly on δ the *charge distribution* in Tl-2223 and Tl-2234 does not change as a function of pressure and hence the charge carrier density n_h of both the inner and outer CuO_2 layers shows a linear dependence on δ. This behavior is depicted in the insets of Fig. 2. How δ depends on the applied pressure p is beyond the scope of this simple model.

Once the charge distribution among the inequivalent CuO_2 layers is calculated, the empirically found parabolic dependence of T_c upon n_h may be used to determine the intrinsic T_c values of each of the CuO_2 layers normalized with respect to $T_{c\rm max}$. This parabolic relation is generally given by[1,2,16]

$$T_c=T_{c\rm max}[1-\beta(n_h-n_{h\rm max})^2], \tag{10}$$

with[1,2] $\beta=82.6$ and $n_{h\rm max}=0.16$. Even though the values of these parameters were obtained from measurements of T_c as

a function of the strontium content z and hence as a function of n_h in the $La_{2-z}Sr_zCuO_4$ system it has been shown by Shafer and Penney[3] that they describe the behavior of other high-T_c superconductors as well. Superconductivity is observed for[3] $0.05<n_h<0.27$ with a maximum in T_c at $n_h=0.16$. Generally, n_h increases linearly with pressure,[17] although, in principle, also $T_{c\max}$, β, and $n_{h\max}$ may change with pressure.

In Fig. 2 the normalized T_c values for the inner and outer CuO_2 layers of Tl-2223 and Tl-2234, which were calculated using Eq. (10), are shown as a function of δ. In Tl-2223 the outer CuO_2 layers become superconducting for δ values between 0.1 and 0.6, reaching a maximum T_c at $\delta\approx 0.35$. For values of δ above 0.6 the inner CuO_2 layer becomes superconducting while the outer CuO_2 layers are not superconducting anymore. In Tl-2234 the outer CuO_2 layers behave in a similar way as in Tl-2223. This is not so surprising since the charge carrier density n_h of these layers is almost not influenced by the addition of an inner CuO_2 layer together with a single Ca layer. On the other hand, the amount of charge carriers originally available in the single inner CuO_2 layer in Tl-2223 has to be distributed equally among the two inner CuO_2 layers in Tl-2234. As a result these inner CuO_2 layers cannot be doped sufficiently in order to become intrinsically superconducting.

B. Model of Haines and Tallon

The crystal structures of high-T_c superconductors are usually considered to be *ionic*.[18] This implies that charges can be assigned to each of the constituent cations (metal ions) and anions (oxygen ions) which are represented as point charges. The *sheet-charge model* of Di Stasio, Müller, and Pietronero[14] has therefore been modified to a *point-charge model* by Haines and Tallon[15] simply by replacing the electrostatic energy as defined by Di Stasio *et al.*[14] [see Eq. (4)] with the Madelung energy

$$U_{\mathrm{Mad}}=\frac{e^2}{2}\sum_{\mathbf{R}}\sum_{\mathbf{q},\mathbf{q}'}\frac{Z_qZ_{q'}}{|\mathbf{R}+\mathbf{q}-\mathbf{q}'|}=\frac{e^2}{2S}\sum_{\mathbf{q},\mathbf{q}'}Z_qZ_{q'}\left(-\frac{S_{qq'}}{2}\right), \tag{11}$$

where e is the electron charge, Z_q is the charge at site $\mathbf{q}$, S is the average Wigner-Seitz radius, and

$$S_{qq'}=-2\sum_{\mathbf{R}}\frac{S}{|\mathbf{R}+\mathbf{q}-\mathbf{q}'|} \tag{12}$$

is the Madelung sum which is calculated using standard techniques.[19] To calculate the Madelung sums for Tl-2223 and Tl-2234 the atomic positions given by Kasowski *et al.*[20] were used. Given the lattice parameters $a=3.850$ Å and $c=35.88$ Å for Tl-2223 (Ref. 20) and $a=3.853$ Å and $c=41.98$ Å for Tl-2234,[21] the average Wigner-Seitz radius of these compounds is found to be 1.495 Å and 1.479 Å, respectively.

Since the affinity of the charge carriers within the CuO_2 layers to reside on the oxygen sites [i.e., the O(1) sites of the inner CuO_2 layer(s) or the O(2) sites of the outer CuO_2 layers] is probably larger than the affinity to reside on the copper sites [i.e., the Cu(1) sites of the inner CuO_2 layer(s) or the Cu(2) sites of the outer CuO_2 layers], it is assumed that a *fraction* f of the available number of charge carriers resides on the copper sites while a *fraction* $1-f$ resides on the oxygen sites. Assigning to the rest of the atomic constituents their nominal valencies, the charge distribution given in Table I and Table II is obtained for Tl-2223 and Tl-2234, respectively. The Madelung energy as given by Eq. (11) can then be simplified considerably as shown by Haines and Tallon,[15]

$$U_{\mathrm{Mad}}=\frac{e^2\delta}{2\epsilon S}[b_0+b_1\delta+(b_2+b_3\delta)x+b_4\delta x^2], \tag{13}$$

where the coefficients b_i depend on f and $S_{qq'}$. Again the dielectric constant ϵ enters Eq. (13) since not all electron bands are taken into account in the calculation of the band energy. These bands act as an effective medium. In Appendix A and Appendix B expressions for these coefficients are given for Tl-2223 and Tl-2234, respectively,[22] while in Table III numerical values are given in the case $f=0$.

Since the Madelung energy is calculated with respect to its value at $x=0$ for any value of f, the constant terms in the coefficients b_0 and b_1 may be neglected.

Increasing the value of f for the given set of parameters tends to decrease the amount of charge transferred to the inner CuO_2 layer in Tl-2223 considerably, hence increasing the charge on the outer CuO_2 layers. In Tl-2234, on the other hand, the charge distribution is not very sensitive to the value of f.

The distribution of charge between the inner and outer CuO_2 layers may now be calculated by minimizing the total energy $U_{\mathrm{tot}}=U_b+U_{\mathrm{Mad}}$ with respect to the fraction x. The

TABLE I. Ionic charge distribution in Tl-2223.

Layer	Atom	Charge	Atom numbering
	Tl	$3-\frac{1}{2}\delta$	1, 2
	O(4)	-2	3, 4
	Ba	2	5, 6
	O(3)	-2	7, 8
	Ca	2	15, 16
Inner	Cu(1)	$2+fx\delta$	17
Inner	O(1)	$-2+\frac{1}{2}(1-f)x\delta$	18, 19
Outer	Cu(2)	$2+\frac{1}{2}f(1-x)\delta$	9, 10
Outer	O(2)	$-2+\frac{1}{4}(1-f)(1-x)\delta$	11, 12, 13, 14

TABLE II. Ionic charge distribution in Tl-2234.

Layer	Atom	Charge	Atom numbering
	Tl	$3-\frac{1}{2}\delta$	1, 2
	O(4)	-2	3, 4
	Ba	2	5, 6
	O(3)	-2	7, 8
	Ca	2	15, 16, 17
Inner	Cu(1)	$2+\frac{1}{2}fx\delta$	18, 19
Inner	O(1)	$-2+\frac{1}{4}(1-f)x\delta$	20, 21, 22, 23
Outer	Cu(2)	$2+\frac{1}{2}f(1-x)\delta$	9, 10
Outer	O(2)	$-2+\frac{1}{4}(1-f)(1-x)\delta$	11, 12, 13, 14

TABLE III. The coefficients b_i in Eq. (13) for Tl-2223 and Tl-2234 in the case $f=0$, where f is the *fraction* of the available number of charge carriers that reside on the copper sites. Neglecting the constant terms in the coefficients b_0 and b_1, as explained in the text, it follows immediately from the expressions given in Appendix A and Appendix B that for $f=0$ both b_0 and b_1 are zero.

	Tl-2223	Tl-2234
b_0	0.0000	0.0000
b_1	0.0000	0.0000
b_2	-0.6721	-0.4882
b_3	1.0725	1.0593
b_4	0.3819	0.9229

value of $x_{\min}$, corresponding to the minimum must, of course, satisfy the condition $0 \leqslant x_{\min} \leqslant 1$. If $\partial^2 U_{\rm tot}/\partial x^2 > 0$, it is given by

$$x_{\min} = \frac{1 - A_p(b_2/\delta + b_3)}{3 + 2A_p b_4} \quad \text{for } n=3,$$

$$x_{\min} = \frac{1 - A_p(b_2/\delta + b_3)}{2(1 + A_p b_4)} \quad \text{for } n=4, \tag{14}$$

where

$$A_p = \frac{m_e e^2}{\hbar^2}\,\frac{a^2}{\pi S}\,\frac{m^*/m_e}{\epsilon}. \tag{15}$$

However, if $\partial^2 U_{\rm tot}/\partial x^2 < 0$, the energy minimum occurs at $x=0$ and/or $x=1$. The same values are also found if $x_{\min}$ given by Eq. (14) lies outside the range $0 \leqslant x \leqslant 1$.

In the insets of Fig. 3 the variation in charge on the inner and outer CuO_2 layers of Tl-2223 and Tl-2234 is given as a function of δ in the case where all the holes reside on the oxygen sites ($f=0$) as suggested by photoemission experiments,[23–25] again taking $(m^*/m_e)/\epsilon \simeq 0.33$. Contrary to the results of the model of Di Stasio, Müller, and Pietronero,[14] the insets of Fig. 3 clearly show that for small values of δ all of the charge is confined to the inner CuO_2 layer(s). Transfer to the outer CuO_2 layers occurs only for $\delta > 0.23$ and $\delta > 0.13$ in Tl-2223 and Tl-2234, respectively, while at the same time the amount of charge on the inner CuO_2 layer(s) decreases. Assuming at ambient pressure a δ value of 0.45 for Tl-2223 as well as for Tl-2234, it appears that in Tl-2223 the charge distribution is almost homogeneous in agreement with ^{63}Cu and ^{17}O NMR measurements[26,27] and that the CuO_2 layers are close to optimal doping. Interestingly, with increasing doping the hole concentration on the inner CuO_2 layer decreases, while for the outer CuO_2 layers it increases; i.e., the inner layer appoaches optimal doping from the overdoped side while the outer layers approach from the underdoped side. In contrast, in Tl-2234 the charge distribution is clearly inhomogeneous where the inner CuO_2 layers are underdoped while the outer CuO_2 layers are overdoped. In Fig. 3 the normalized T_c values for the inner and outer CuO_2 layers of Tl-2223 and Tl-2234, which again were calculated using Eq. (10), are shown as a function of δ.

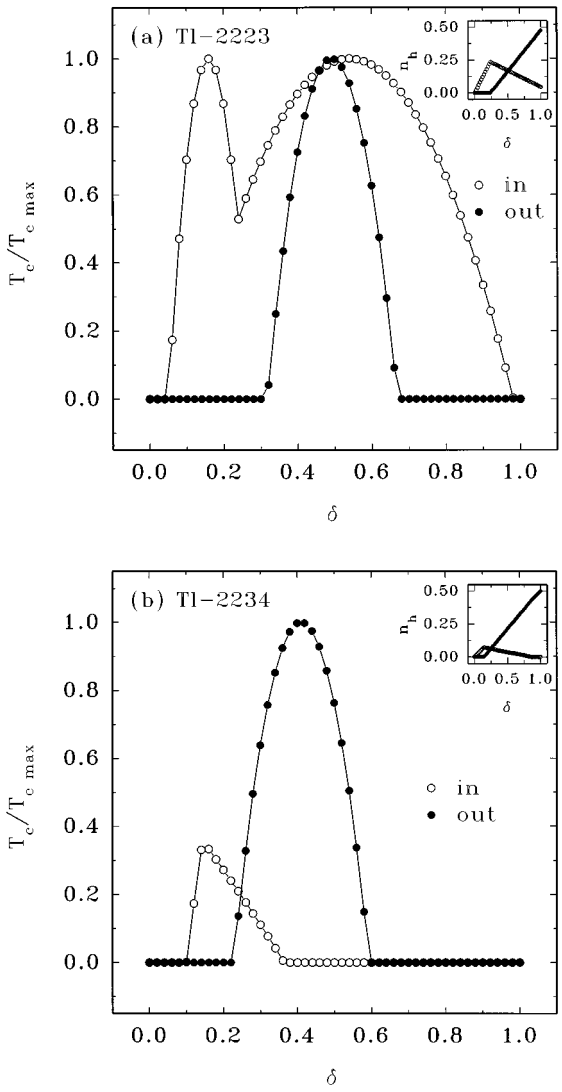

FIG. 3. Normalized T_c values for the inner and outer CuO_2 layers as a function of the total number δ of holes transferred from the TlO charge reservoir layers to the CuO_2 layers in (a) Tl-2223 and (b) Tl-2234 based on Eq. (10) and the calculated charge distribution as shown in the insets taking $(m^*/m_e)/\epsilon \simeq 0.33$.

In the present model the intrinsic $T_c/T_{c\max}$ values for the inner and outer CuO_2 layers may be calculated using Eqs. (3), (10), and (14) where $x_{\min}$ is substituted for x. In this calculation the free parameter A_p determines the relative contribution of the electrostatic and band energies. For $(m^*/m_e)/\epsilon$ the values of 0.04, 0.016, and 0.008 are considered. On the left-hand side of Figs. 4 and 5 the intrinsic T_c's of the inner and outer CuO_2 layers are shown normalized with respect to $T_{c\max}$. Since it was found previously[17,28] that the main effect of pressure is an increase of the charge carrier density of the CuO_2 layers, $\delta \sim p$; hence the δ axis can be replaced by a pressure axis. The right-hand side of Figs. 4 and 5 shows (open squares) the maximum value of $T_c/T_{c\max}$ of the inner and outer CuO_2 layers corresponding to the case that the CuO_2 layers are decoupled (*two-dimensional* case). It also shows $T_c/T_{c\max}$ (solid squares) for the case where the CuO_2 layers are coupled in the

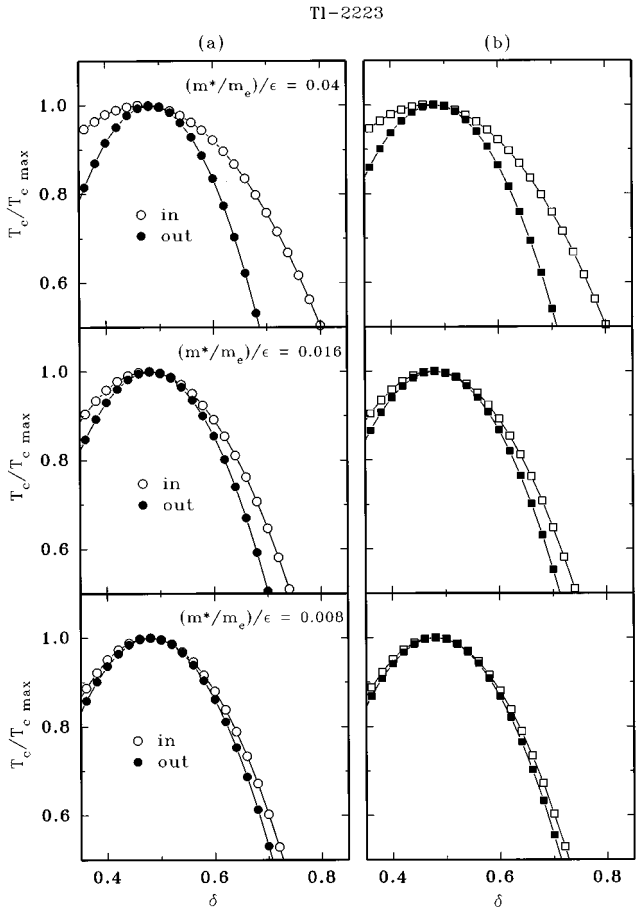

FIG. 4. (a) Intrinsic $T_c/T_{c\max}$ values for the inner and outer CuO_2 layers in Tl-2223, calculated using the model of Haines and Tallon (Ref. 15) for $(m^*/m_e)/\epsilon = 0.04, 0.016$, and 0.008. (b) Effective $T_c/T_{c\max}$ values for the compound as a whole, calculated in the case where (open squares) the CuO_2 layers are decoupled (*two-dimensional* case) and (solid squares) the CuO_2 layers are coupled in the Cooper–de Gennes limit (*three-dimensional* case). All the charge carriers are assumed to reside on the oxygen sites ($f=0$).

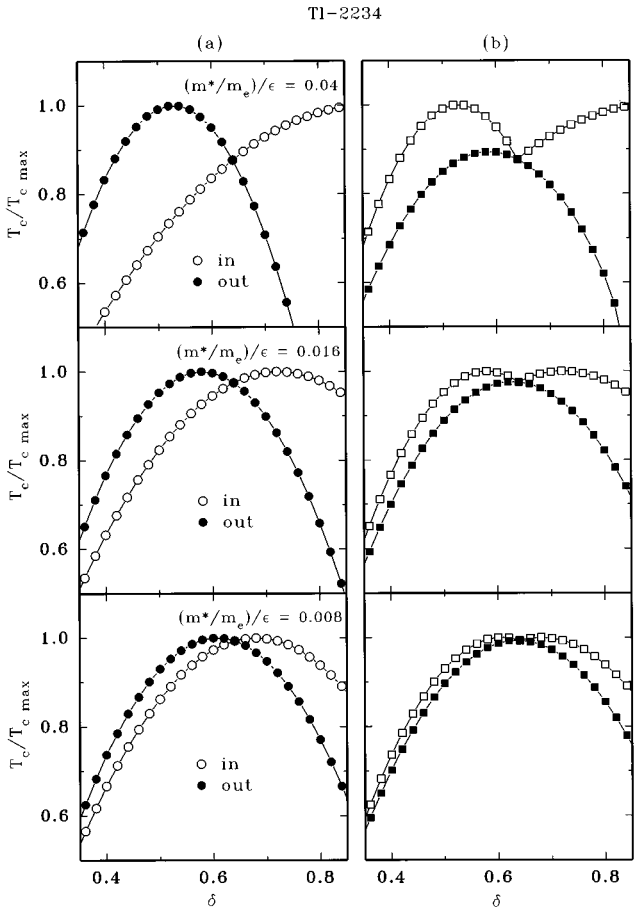

FIG. 5. (a) Intrinsic $T_c/T_{c\max}$ values for the inner and outer CuO_2 layers in Tl-2234, calculated using the model of Haines and Tallon (Ref. 15) for $(m^*/m_e)/\epsilon = 0.04, 0.016$, and 0.008. (b) Effective $T_c/T_{c\max}$ values for the compound as a whole, calculated in the case where (open squares) the CuO_2 layers are decoupled (*two-dimensional* case) and (solid squares) the CuO_2 layers are coupled in the Cooper–de Gennes limit (*three-dimensional* case). All the charge carriers are assumed to reside on the oxygen sites ($f=0$).

Cooper–de Gennes limit (*three-dimensional* case). To calculate an effective T_c in this limit a simple BCS-type relation is used:

$$T_c = 1.14\Theta_D \exp(-1/\lambda), \tag{16}$$

where λ is the coupling parameter of the Cooper pairs. For the Debye temperature Θ_D a value of 500 K is taken. After calculating λ from T_c for both the inner and outer CuO_2 layers, an effective coupling parameter $\lambda_{\rm eff}$ can be obtained using the equation[29]

$$\lambda_{\rm eff} = \frac{\Sigma_i d_i \mathcal{D}_i \lambda_i}{\Sigma_i d_i \mathcal{D}_i}, \tag{17}$$

where d_i is the thickness of the ith CuO_2 layer, $\mathcal{D}_i$ is the density of states of that layer, and λ_i is the corresponding coupling parameter. If the density of states and the thickness are taken to be the same for all CuO_2 layers, then Eq. (17) reduces to a simple average

$$\lambda_{\rm eff} = \frac{\Sigma_{i=1}^{n} \lambda_i}{n}, \tag{18}$$

which can be substituted for λ in Eq. (16) to give an effective T_c in the Cooper–de Gennes limit.[30]

III. SAMPLE PREPARATION AND CHARACTERIZATION

As already discussed, and shown in Fig. 1, Tl-2223 has three ($n=3$) CuO_2 layers per half unit cell while Tl-2234 has four ($n=4$). It is this large amount of stacked CuO_2 layers that makes the preparation of single-phase Tl-2223 and Tl-2234 material difficult. An additional element[31] is the control of oxygen partial pressure during annealing.

The Tl-2223 sample studied in this work was prepared following the method described by Liu *et al.*[31] Their procedure involves synthesizing a material with nominal stoichiometry $Tl_{1.6}Ba_2Ca_{2.4}Cu_3O_{10+y}$ by thoroughly mixing appropriate amounts of high-purity Tl_2O_3, BaO_2, CaO, and CuO powders using a mortar and a pestle. This mixture is then pressed into a pellet (10 mm in diameter and 3 mm in

thickness) under a pressure of 0.5 GPa and wrapped in gold foil to prevent loss of thallium at elevated temperatures during sintering in a furnace at 910 °C for 3 h in oxygen. After sintering, the furnace is cooled to room temperature at a rate of 5 °C/min. The as-sintered sample with a zero-resistance temperature of 119 K was then wrapped in gold foil, encapsulated in an evacuated ($\sim 10^{-4}$ Torr) quartz tube, and annealed at 750 °C for 10 days. This procedure resulted in an increase of the zero-resistance temperature to 125.1 K. The resulting sample was then annealed in an oxygen-nitrogen atmosphere with an oxygen partial pressure of 0.2% at 600 °C for 2 h and rapidly quenched into liquid nitrogen. This annealing optimized the hole concentration n_h and at ambient pressure a T_c of 128.5 K (extrapolated value from the T_c vs p curve) was reached in the Tl-2223 sample. The fact that this sample was optimally doped could easily be confirmed by further oxygenating a similarly prepared sample in an oxygen-nitrogen atmosphere with a partial oxygen pressure of 2% which showed a lower T_c. Analyzing the powder x-ray diffraction (XRD) patterns of the Tl-2223 sample studied in this work using a Philips PW1710 x-ray diffractometer with Cu $K\alpha$ radiation (1.54 Å) almost all of the XRD peaks in the sample could be assigned to the Tl-2223 phase, showing no dominant impurity phase. Neutron diffraction experiments showed furthermore that the sample was single phased. The Tl-2234 sample with nominal composition $Tl_{1.7}Ba_2Ca_{3.3}Cu_4O_{12+y}$ was prepared in a similar way starting with a $Tl_{1.5}Ba_2Ca_{4.5}Cu_5O_{14+y}$ precursor. XRD showed that the Tl-2234 sample with, at ambient pressure, a T_c between 113 K (extrapolated value from the T_c vs p curve) and 115 K (determined from resistance measurements at ambient pressure) was nearly phase pure with only a slight fraction of Tl-2223. In resistance measurements at ambient pressure this small amount of Tl-2223 results in a secondary superconducting transition around 123 K. In ac-susceptibility measurements a sharp transition was observed at 114 K together with a very small diamagnetic signal around 122 K. For high-pressure experiments, however, such small amounts of the sample material are needed that the Tl-2223 phase is practically absent; i.e., this phase is not visible in the resistance measurements under pressure.

IV. EXPERIMENTAL DETAILS

Pressure is generated and applied to the samples using a cryogenic diamond anvil cell[32] (DAC) made of hardened beryllium copper alloy (Berylco 25) and can be simply changed by turning a knob at the top of the cryostat. By doing this, two parallel aligned diamonds are pushed towards each other (see Fig. 6) using a lever-based system. In this work 16-sided diamond anvils are used with a culet (high-pressure face) diameter of typically 0.9 mm. The type-I diamonds (containing small amounts of nitrogen platelets, enhancing their strength) are cut according to the standard Drukker design and are single beveled under an angle of 5° in order to reduce pressure gradients across the edges of the culet. This is done to prevent breakage of the electrical leads for resistivity measurements under pressure. Under such conditions resistive measurements up to pressures as high as 21 GPa are possible within this DAC.

In order to measure the applied pressure *in situ*, close to the superconducting transition of the samples, the ruby fluorescence method is used. For this purpose several small pieces of ruby are pressurized together with the sample. The fluorescence spectrum of such a ruby grain is obtained by focussing an Ar^+-ion laser (operating at 514.5 nm) on it with the aid of a camera system and is then detected with a 1403 spectrometer from SPEX Industries.

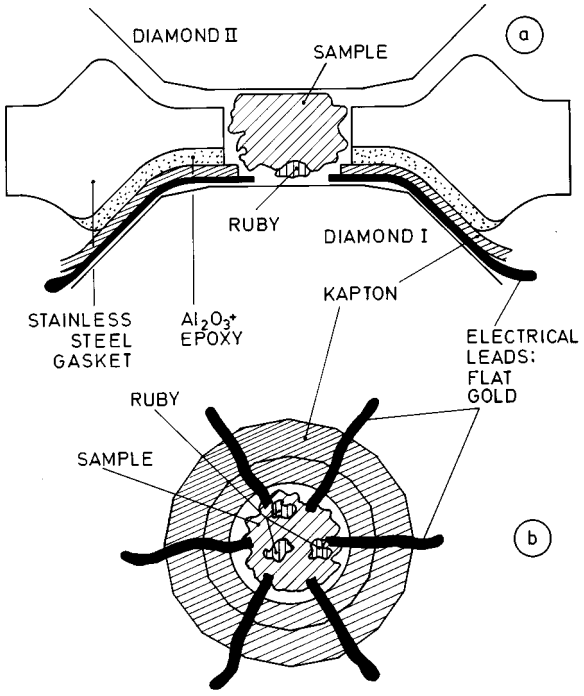

FIG. 6. (a) Cross-section and (b) bottom view of the sample space in the DAC before compression. As shown, the gasket is insulated from the flattened gold wires using a thin Kapton foil glued to the gasket using a mixture of Al_2O_3 and epoxy. In the center of the gasket a hole with a diameter of 300 μm is drilled which serves as sample space and confines the high-pressure generated in the DAC. Although strictly only four electrical leads are needed to perform four-point resistance measurements, six leads are positioned in order to have two spare ones. The small pieces of ruby are used to determine the pressure in the cell.

Ruby has two distinct fluorescence lines, known as the R_1 and R_2 lines, and their positions depend not only on the applied pressure but also on the temperature. After correction for the temperature-induced shift of the ruby R_1 fluorescence line[33] the calibration of Mao *et al.*[34] is used to determine the applied pressure.

During the superconducting transition of Tl-2223 and Tl-2234 the pressure in the sample space is measured at temperatures close to T_c. The temperature of the sample is measured using a standard platinum resistor placed in a copper block in which diamond II is mounted. Since both copper and diamond are good thermal conductors, thermal gradients between the platinum resistor and the sample are certainly less than 0.5 K. This value is obtained from the thermal hysteresis observed in the superconducting transitions while cycling the temperature up and down.

The sample can be cooled by flowing liquid helium through a heat exchanger while its temperature can be increased by passing a current through a constantan wire

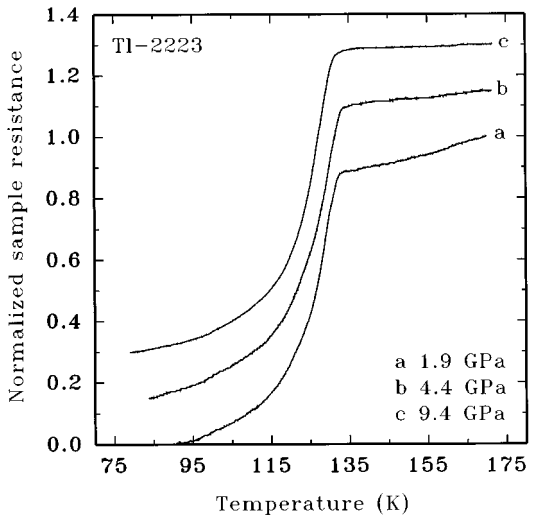

FIG. 7. Superconducting transitions of Tl-2223 at different pressures. After subtraction of the residual resistance the superconducting transitions are normalized with respect to their values at 170 K.

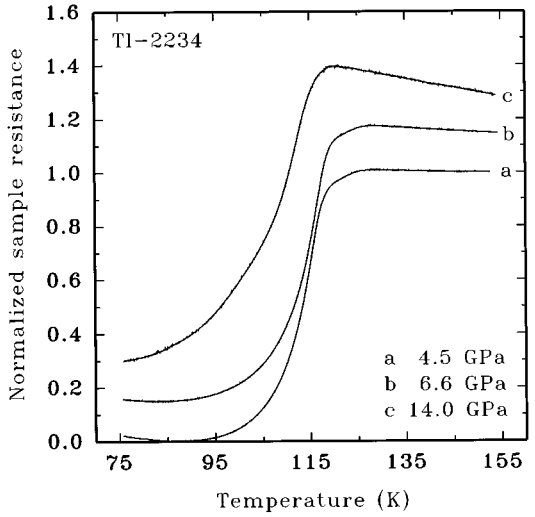

FIG. 8. Superconducting transitions of Tl-2234 at different pressures. After subtraction of the residual resistance the superconducting transitions are normalized with respect to their values at 150 K.

heater. In this way the temperature of the sample can be varied continuously between 10 K and 300 K under control of a temperature regulator at an average rate of 0.5 K/min.

The superconducting transition temperature T_c of the sample is determined resistively using the standard four-probe technique which was improved for high-pressure experiments by van Eenige *et al.*[35] On top of diamond I six flattened gold wires with a diameter of 25 μm are positioned although strictly only four are needed (the other two are spares). Their ends lie within a radius of 150 μm from the center of the diamond anvil. A 100 μm thick stainless steel gasket is placed on top of the gold wires. In the center of the gasket a hole with a diameter of 300 μm is drilled which serves as sample space. For insulation a 13 μm thick Kapton foil is glued to the side facing the wires using a 1 : 1 mixture of Al_2O_3 powder with an average grain size of 0.05 μm and epoxy adhesive. The sample space is completely filled with sample material. The main purpose of the gasket is to support the diamond anvils and to sustain the quasihydrostatic pressures generated in the DAC. The temperature dependence of the four-point resistance, $R(T)$, of the samples is measured with a Keithley 197 A multimeter using a current of 1.8 mA.

V. EXPERIMENTAL RESULTS AND DISCUSSION

In Figs. 7 and 8 typical superconducting transitions of the Tl-2223 and Tl-2234 samples are shown at different pressures. Under pressure the polycrystalline samples break up into smaller grains. Since the intergrain boundaries are not superconducting, they are responsible for residual resistances observed at temperatures below T_c. After subtraction of these residual resistances, the superconducting transitions are normalized with respect to their values at 170 K for the Tl-2223 sample and at 150 K for the Tl-2234 sample. The superconducting transition temperature T_{ct} is defined as the intersection of the tangent through the inflection point of the resistive transition with a straight-line fit of the normal state just above the transition. At low pressures the rate at which T_c increases with pressure is found to be 1.75 K/GPa and 2.0 K/GPa for Tl-2223 and Tl-2234, respectively. As the applied pressure is increased further, T_c continues to increase until it reaches a maximum value of 133 K at 4.2 GPa in Tl-2223 and of 120 K at 6.6 GPa in Tl-2234. At still higher pressures T_c starts to decrease. During this decrease a rather abrupt change in the slope is observed at 12.0 GPa in Tl-2223 and at 10.5 GPa in Tl-2234.

This behavior is quite different from that observed in the $n=1$ and $n=2$ layered high-T_c superconductors. In most of these compounds, T_c as a function of pressure is reasonably well described by a simple parabola.[7,8,36] For example in $Y_2Ba_4Cu_7O_{15.32}$ (Y-247) van Eenige *et al.*[37] observed such a parabolic behavior over a wide temperature and pressure range. They showed that T_c first increases from its ambient value of 80 K to 108 K and then drops down to 50 K at 21 GPa. Incidentally, in Y-247 at still higher pressures T_c does not follow the parabola anymore for reasons related to the discussion below.

For Tl-2223 (see Fig. 9) clearly two regimes are present. Below 12.0 GPa the data points follow one parabola while above 12.0 GPa they follow another parabola which has a slightly lower $T_{c\max}$ and a larger width. The parabolas shown in the figure are the result of least-squares fits to selections of the data points as indicated in Table IV. Both parabolas have maxima at approximately the same pressure. These experimental results show qualitatively the same behavior as the calculation based on the model of Haines and Tallon[15] presented in Fig. 4. A possible interpretation of the experiment is as follows. At low pressure the T_c observed is the intrinsic T_c of the *outer* CuO_2 layers in which the charge carrier concentration has a strong pressure dependence and where a clear parabolic behavior for $T_c(p)$ occurs. At the highest pressures the effect of the *inner* CuO_2 layer dominates. As seen in the inset of Fig. 3(a) $\partial n_h/\partial p$ of these layers is smaller and hence the parabola is broader. Clearly the observed behavior in Tl-2223 is consistent with the predictions of the model of Haines and Tallon[15] for the decoupled case

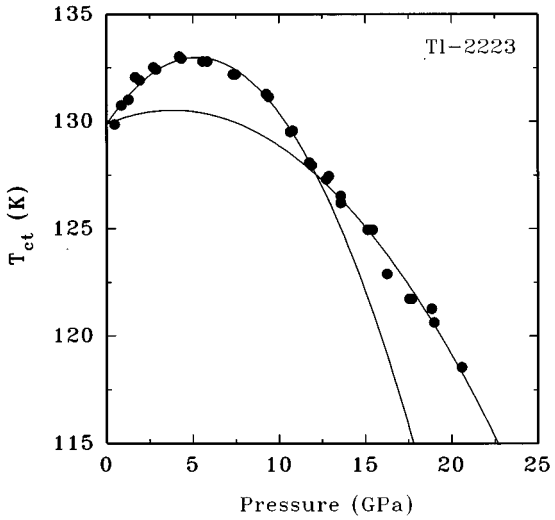

FIG. 9. Pressure dependence of the superconducting transition temperature T_{ct} of Tl-2223 up to 21 GPa. The lines are fits to the experimental results using the parabolic equation $T_c = a_0 + a_1 p + a_2 p^2$. The fits were done separately for pressures below and above 12.0 GPa. The fit parameters are given in Table IV.

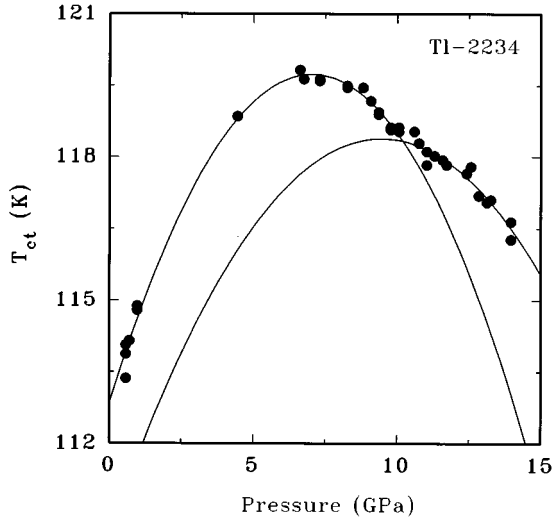

FIG. 10. Pressure dependence of the superconducting transition temperature T_{ct} of Tl-2234 up to 14 GPa. The lines are fits to the experimental results using the parabolic equation $T_c = a_0 + a_1 p + a_2 p^2$. The fits were done separately for pressures below and above 10.5 GPa. The fit parameters are given in Table IV.

as shown in Fig. 4. In particular the model predicts a nearly homogeneous charge distribution between the inner and outer CuO_2 layers and hence the maxima for the inner and outer CuO_2 layers occur at approximately the same pressure.

For Tl-2234 (see Fig. 10) also two regimes are present. Below 10.5 GPa the data points follow one parabola and above 10.5 GPa they follow another parabola which has a slightly lower $T_{c\max}$ and a somewhat larger width. The parabolas shown in the figure are the result of least-squares fits to selections of the data points as indicated in Table IV. The positions of the maxima of the parabolas differ by approximately 4 GPa. These experimental results show qualitatively the same behavior as the calculation presented in Fig. 5 and can be interpreted as follows. At low pressure the observed T_c is the intrinsic T_c of the *outer* CuO_2 layers in which the charge carrier concentration has a strong pressure dependence and where a clear parabolic behavior for $T_c(p)$ occurs. At the highest pressures the effect of the *inner* CuO_2 layers dominates. As seen in the inset of Fig. 3(b) $\partial n_h / \partial p$ of these layers is smaller and hence the parabola is broader. Clearly the observed behavior in Tl-2234 is consistent with the predictions of the model of Haines and Tallon[15] for the decoupled case as shown in Fig. 5. In particular the model predicts an inhomogeneous charge distribution between the inner and outer CuO_2 layers and hence the maxima for the inner and outer CuO_2 layers occur at different pressures.

Although the model of Haines and Tallon[15] is consistent with the present experiment, it must be emphasized that other interpretations are possible. For example the kink in $\partial T_c / \partial p$ might be due to a kink in $\partial n_h / \partial p$ for a single CuO_2 layer.

VI. CONCLUSION

The pressure dependence of Tl-2223 up to 21 GPa and of Tl-2234 up to 14 GPa has been measured. For both Tl-2223 and Tl-2234 a clear deviation from the parabolic pressure dependence has been observed in the T_c vs p curves seen in many other compounds. This deviation is ascribed to the presence of two different kinds of CuO_2 layers, viz., the

TABLE IV. The experimental results shown in Figs. 9 and 10 are fitted with the parabolic function $T_c = a_0 + a_1 p + a_2 p^2$. The pressure p is expressed in GPa and the superconducting critical temperature T_c in K.

Fit parameter	Tl-2223		Tl-2234	
	$p < 12.0$ GPa	$p > 12.0$ GPa	$p < 10.5$ GPa	$p > 10.5$ GPa
a_0 (K)	129.9	129.9[a]	112.8	110.1
a_1 (K/GPa)	1.190	0.3362	1.959	1.756
a_2 (K/GPa^2)	-0.1139	-0.0437	-0.1392	-0.09276

[a]Constrained during the fit to be smaller or equal to a_0 ($p < 12.0$ GPa).

inner and outer CuO_2 layers. Due to the weak proximity coupling between these layers, T_c is determined by the CuO_2 layer with the highest intrinsic T_c. This is consistent with the large mass anisotropy of the thallium- and mercury-based compounds with $n>2$. The experimental findings obtained in this work are in qualitative agreement with the point-charge model of Haines and Tallon.[15] Clearly, to make a quantitative comparison, also the *intrinsic* (i.e., not due to change in charge carrier concentration) pressure dependence of T_c should be taken into account.[38–40] Since this introduces new parameters which are not all known, it is left as a subject for future work.

ACKNOWLEDGMENTS

The authors wish to thank Dr. E. N. van Eenige for valuable discussions. Also the technical assistance of in particular W. Rave-Koot from the Geology department and of Ing. K. Heeck is gratefully appreciated. This work is part of the research program of the Stichting voor Fundamenteel Onderzoek der Materie (FOM) which is financially supported by NWO. The work in Lower Hutt was in part financially supported by the New Zealand Foundation for Research in Science and Technology and the Electricity Corporation of New Zealand.

[1] J. L. Tallon, C. Bernhard, H. Shaked, R. L. Hitterman, and J. D. Jorgensen, Phys. Rev. B **51**, 12 911 (1995).

[2] J. L. Tallon and J. R. Cooper, in *Advances in Superconductivity V*, edited by Y. Bando and H. Yamauchi (Springer-Verlag, Tokyo, 1993), p. 339.

[3] M. W. Shafer and T. Penney, Eur. J. Solid State Inorg. Chem. **27**, 191 (1990).

[4] J. M. Wheatley, T. C. Hsu, and P. W. Anderson, Nature (London) **333**, 121 (1988).

[5] C. C. Tsuei, D. M. Newns, C. C. Chi, and P. C. Pattnaik, Phys. Rev. Lett. **65**, 2724 (1990).

[6] D. M. Newns, C. C. Tsuei, R. P. Huebener, P. J. M. van Bentum, P. C. Pattnaik, and C. C. Chi, Phys. Rev. Lett. **73**, 1695 (1994).

[7] R. J. Wijngaarden and R. Griessen, in *Studies of High Temperature Superconductors*, edited by A. V. Narlikar (Nova Science, New York, 1989), Vol. 2, p. 29.

[8] J. S. Schilling and S. Klotz, in *Physical Properties of High Temperature Superconductors*, edited by D. M. Ginsberg (World Scientific, Singapore, 1992), Vol. III, p. 84.

[9] H. Takahashi and N. Môri, in *Studies of High Temperature Superconductors*, edited by A. V. Narlikar (Nova Science, New York, 1995), Vol. 16, p. 1.

[10] I. V. Berman, N. B. Brandt, Yu. P. Kurkin, E. A. Naumova, I. L. Romashkina, V. I. Sidorov, A. I. Akimov, V. I. Gapal'skaya, and E. K. Stribuk, JETP Lett. **49**, 769 (1989).

[11] W. H. Fietz, C. A. Wassilew, H. A. Ludwig, B. Obst, C. Politis, M. R. Dietrich, and H. Wühl, High Press. Res. **4**, 423 (1990).

[12] R. Kubiak, K. Westerholt, G. Pelka, H. Bach, and Y. Khan, Physica C **166**, 523 (1990).

[13] D. D. Berkley, E. F. Skelton, N. E. Moulton, M. S. Osofsky, W. T. Lechter, V. M. Browning, and D. H. Liebenberg, Phys. Rev. B **47**, 5524 (1993).

[14] M. Di Stasio, K. A. Müller, and L. Pietronero, Phys. Rev. Lett. **64**, 2827 (1990).

[15] E. M. Haines and J. L. Tallon, Phys. Rev. B **45**, 3172 (1992).

[16] R. P. Gupta and M. Gupta, Phys. Rev. B **51**, 11 760 (1995).

[17] R. J. Wijngaarden, J. J. Scholtz, E. N. van Eenige, and R. Griessen, in *Frontiers of High Pressure Research*, Vol. 286 of NATO Advanced Study Institute, Series B: Physics, edited by H. D. Hochheimer and R. D. Etters (Plenum Press, New York, 1992), p. 399, and references therein.

[18] J. Kondo, in *Mechanisms of Superconductivity*, edited by Y. Muto [Jpn. J. Appl. Phys. Series 7 (1992)], p. 301.

[19] H. L. Skriver, in *The LMTO Method: Muffin-Tin Orbitals and Electronic Structure*, edited by M. Cardona and P. Fulde (Springer-Verlag, Berlin, 1984).

[20] R. V. Kasowski, W. Y. Hsu, and F. Herman, Phys. Rev. B **38**, 6470 (1988).

[21] M. Kikuchi, S. Nakajima, Y. Syono, K. Hiraga, T. Oku, D. Shindo, N. Kobayashi, H. Iwasaki, and Y. Muto, Physica C **158**, 79 (1989).

[22] See AIP Document No. E-PAPS: E-PRBMD-54-10175-0.254 MB for expressions for the b_i coefficients for TI-2223 and TI-2234, respectively. E-PAPS document files may be retrieved free of charge from our FTP server (http://www.aip.org/epaps/epaps.html). For further information: e-mail: paps@aip.org or fax: 516-576-2223.

[23] J. A. Yarmoff, D. R. Clarke, W. Drube, U. O. Karlsson, A. Taleb-Ibrahimi, and F. J. Himpsel, Phys. Rev. B **36**, 3967 (1987).

[24] N. Nücker, J. Fink, J. C. Fuggle, P. J. Durham, and W. M. Temmerman, Phys. Rev. B **37**, 5158 (1988).

[25] A. J. Arko, R. S. List, R. J. Bartlett, S.-W. Cheong, Z. Fisk, J. D. Thompson, C. G. Olson, A.–B. Yang, R. Liu, C. Gu, B. W. Veal, J. Z. Liu, A. P. Paulikas, K. Vandervoort, H. Claus, J. C. Campuzano, J. E. Schirber, and N. D. Shinn, Phys. Rev. B **40**, 2268 (1989).

[26] Z. P. Han, R. Dupree, R. S. Liu, and P. P. Edwards, Physica C **226**, 106 (1994).

[27] A. P. Howes, R. Dupree, Z. P. Han, R. S. Liu, and P. P. Edwards, Phys. Rev. B **47**, 11 529 (1993).

[28] M. Kosuge, T. Maeda, K. Sakuyama, T. Miyatake, N. Koshizuka, H. Yamauchi, H. Takahashi, C. Murayama, and N. Môri, Phys. Rev. B **45**, 10 713 (1992).

[29] M. G. Karkut, D. Ariosa, J.-M. Triscone, and Ø. Fischer, Phys. Rev. B **32**, 4800 (1985).

[30] In $Y_{0.8}Ca_{0.2}Ba_2Cu_3O_{7-\delta}$ the density of states at the Fermi level has been observed to increase according to $\mathcal{D}=\mathcal{D}_0(1+6.95n_h^2)$. Assuming that this expression is also valid for the CuO_2 layers in the compounds studied in this work implies that the weight of the effective coupling parameter would move towards the more heavily doped layers.

[31] R. S. Liu, J. L. Tallon, and P. P. Edwards, Physica C **182**, 119 (1991).

[32] H. K. Hemmes, A. Driessen, J. Kos, F. A. Mul, R. Griessen, J. Caro, and S. Radelaar, Rev. Sci. Instrum. **60**, 474 (1989).

[33] I. F. Silvera and R. J. Wijngaarden, Rev. Sci. Instrum. **56**, 121 (1985).

[34] H. K. Mao, J. Xu, and P. M. Bell, J. Geophys. Res. **91**, 4673 (1986).

[35] E. N. van Eenige, R. Griessen, R. J. Wijngaarden, J. Karpinski, E. Kaldis, S. Rusiecki, and E. Jilek, Physica C **168**, 482 (1990).

[36] N. Môri, C. Murayama, H. Takahashi, H. Kaneko, K. Kawabata, Y. Iye, S. Uchida, H. Takagi, Y. Tokura, Y. Kubo, H. Sasakura, and K. Yamaya, Physica C **185–189**, 40 (1991).

[37] E. N. van Eenige, R. Griessen, K. Heeck, H. G. Schnack, R. J. Wijngaarden, J.–Y. Genoud, T. Graf, A. Junod, and J. Muller, Europhys. Lett. **20**, 41 (1992).

[38] R. J. Wijngaarden, E. N. van Eenige, J. J. Scholtz, and R. Griessen, Physica C **185–189**, 787 (1991).

[39] J. J. Neumeier and H. A. Zimmermann, Phys. Rev. B **47**, 8385 (1993).

[40] J. J. Neumeier, Physica C **233**, 354 (1994).